Finally, X_{AlCl_3} (saturated) is obtained as

$$X_{AlCl_3} = \frac{(1-x)/M_{NaAlCl_4}}{(x/M_{NaCl}) + 2(1-x)/M_{NaAlCl_4}} \quad (A6)$$

Calculation of Oxide Contents. Suppose that the weight of impure $AlCl_3$ ($W_{AlCl_3} + W_{AlOCl}$) and the weight of pure NaCl ($= W_{NaCl}$) is known. From this the apparent mole fraction, $X_{'AlCl_3'}$, can be calculated.

$$X_{'AlCl_3'} = \frac{(W_{AlCl_3} + W_{AlOCl})/M_{AlCl_3}}{(W_{AlCl_3} + W_{AlOCl})/M_{AlCl_3} + W_{NaCl}/M_{NaCl}} \quad (A7)$$

Suppose further that the true composition of the melt (formed by mixing these chemicals) is known from some experiment. As an example, it can be determined potentiometrically.[44] In this case, the melt is contained in one electrode compartment separated (by a porous borosilicate disk) from a reference melt (saturated with NaCl) in the other electrode compartment. Electrodes of aluminum or carbon are used according to the electrode processes

$$AlCl_4^- + 3e^- \rightleftarrows Al + 4Cl^- \quad (A8)$$

$$Cl_2 + 2e^- \rightleftarrows 2Cl^- \quad (A9)$$

The electrode potential difference, ΔE, is measured, e.g., at 175 °C. The chloride concentration, $[Cl^-]$ in mol L^{-1}, is then given by $[Cl^-] = 10^{(-pCl)}$ where

$$pCl = \Delta E/A + pCl_{satd} \quad (A10)$$

If ΔE is expressed in mV, A can be calculated (from the Nernst equation) as $A = 3\mathcal{F}/(4RT \ln 10) = 118.559$ mV for the aluminum electrodes and as $A = \mathcal{F}/(RT \ln 10) = 88.922$ mV for the carbon electrodes ($\mathcal{F}$ = Faraday's constant). pCl_{satd} is 1.128 (6) at 175 °C.[17] The concentration of $AlCl_4^-$ can be found from the density of the melt[50] and the molar weight, $[AlCl_4^-] \simeq 8.877$ M. From the equilibrium

$$2AlCl_4^- \rightleftarrows Cl^- + Al_2Cl_7^- \quad (A11)$$

with equilibrium constant

$$K = \frac{[Cl^-][Al_2Cl_7^-]}{[AlCl_4^-]^2} = 8.9125 \times 10^{-8} \quad (A12)$$

at 175 °C,[17] the $[Al_2Cl_7^-]$ concentration is found.

The net excess of $[Al_2Cl_7^-]$ or $[Cl^-]$ is calculated as the difference. Assuming 100% purity of NaCl, the real amount of pure $AlCl_3$ is then found.

Finally the true mole fraction X_{AlCl_3} is calculated.

$$X_{AlCl_3} = \frac{W_{AlCl_3}/M_{AlCl_3}}{(W_{AlCl_3}/M_{AlCl_3}) + (W_{NaCl}/M_{NaCl})} \quad (A13)$$

From eq A7 and A13 we obtain

$$\frac{W_{AlOCl}}{W_{AlCl_3}} = \frac{X_{'AlCl_3'} - 1 + (1 - X_{AlCl_3})X_{'AlCl_3'}/X_{AlCl_3}}{1 - X_{'AlCl_3'}} \quad (A14)$$

$$\frac{W_{AlOCl}}{W_{NaAlCl_4}} = \frac{W_{AlOCl}M_{AlCl_3}}{W_{AlCl_3}M_{NaAlCl_4}} \quad (A15)$$

The AlOCl molality is then

$$\frac{W_{AlOCl}}{W_{NaAlCl_4}}\left(\frac{1000}{M_{AlOCl}}\right) \quad (A16)$$

Registry No. NaCl, 7647-14-5; $AlCl_3$, 7446-70-0; $NaAlCl_4$, 7784-16-9.

Contribution from the Department of Chemistry, University of California, Santa Barbara, California 93106

Preparation of Well-Defined Surfaces at Atmospheric Pressure: Studies by Electrochemistry and LEED of Pt(100) Pretreated with Iodine

ANDRZEJ WIECKOWSKI,† STEPHEN D. ROSASCO, BRUCE C. SCHARDT, JOHN L. STICKNEY, and ARTHUR T. HUBBARD*

Received May 24, 1983

Reported here are studies by LEED, Auger spectroscopy, and electrochemistry which show that Pt(100) monocrystal surfaces purposely disordered by electrochemical oxidation and reduction (as in the procedure commonly employed to clean or "activate" Pt electrodes) are restored to an ordered state by programmed heating under an Ar atmosphere containing iodine vapor. A nearly hexagonal, centered-rectangular adlattice of I atoms was formed, containing three I and five Pt atoms in the surface unit cell, $\theta_I = 0.6$, Pt(100)[$c(\sqrt{2}\times 5\sqrt{2})$]R45°-I. Programmed heating of this adlattice led to stepwise desorption of halogen and produced a series of related adlattices. One of these, Pt(100)[$(c\sqrt{2}\times 2\sqrt{2})$]R45°-I, at $\theta_I = 0.50$, is particularly amenable to identification, without LEED, by means of its characteristic cyclic voltammogram for silver electrodeposition. The behavior of each iodine adlattice toward silver electrodeposition and programmed temperature desorption is reported. These atmospheric iodine pretreatment and voltammetric procedures for preparing and verifying a well-defined electrode surface do not require vacuum equipment, although demonstration of the ordered structures in this work employed LEED and related techniques under ultrahigh vacuum. This basic approach should be applicable to a wide range of metals and adsorbates.

Introduction

Studies by LEED and electrochemistry of the molecular structure and composition of electrodeposits on platinum monocrystal surfaces pretreated with iodine vapor have been reported.[1-3] Iodine pretreatment and characterization of the monocrystal electrodes under ultrahigh vacuum allowed exploration of the effect of chemisorbed layer structure on the electrodeposition process[4] and also protected the electrode (and electrodeposit) surfaces from attack by the electrolyte and residual gases.[1-4] A number of interdependencies between surface structure and electrochemical behavior were indicated:

†Permanent address: Department of Chemistry, Warsaw University, Warsaw, Poland.

(1) A. T. Hubbard, J. L. Stickney, S. D. Rosasco, M. P. Soriaga, and D. Song, *J. Electroanal. Chem. Interfacial Electrochem.*, **150**, 165 (1983).
(2) J. L. Stickney, S. D. Rosasco, D. Song, M. P. Soriaga, and A. T. Hubbard, *Surf. Sci.*, **130**, 326 (1983).
(3) J. L. Stickney, S. D. Rosasco, and A. T. Hubbard, *J. Electrochem. Soc.*, in press.
(4) J. L. Stickney, S. D. Rosasco, B. C. Schardt, and A. T. Hubbard, *J. Phys. Chem.*, in press.

0020-1669/84/1323-0565$01.50/0

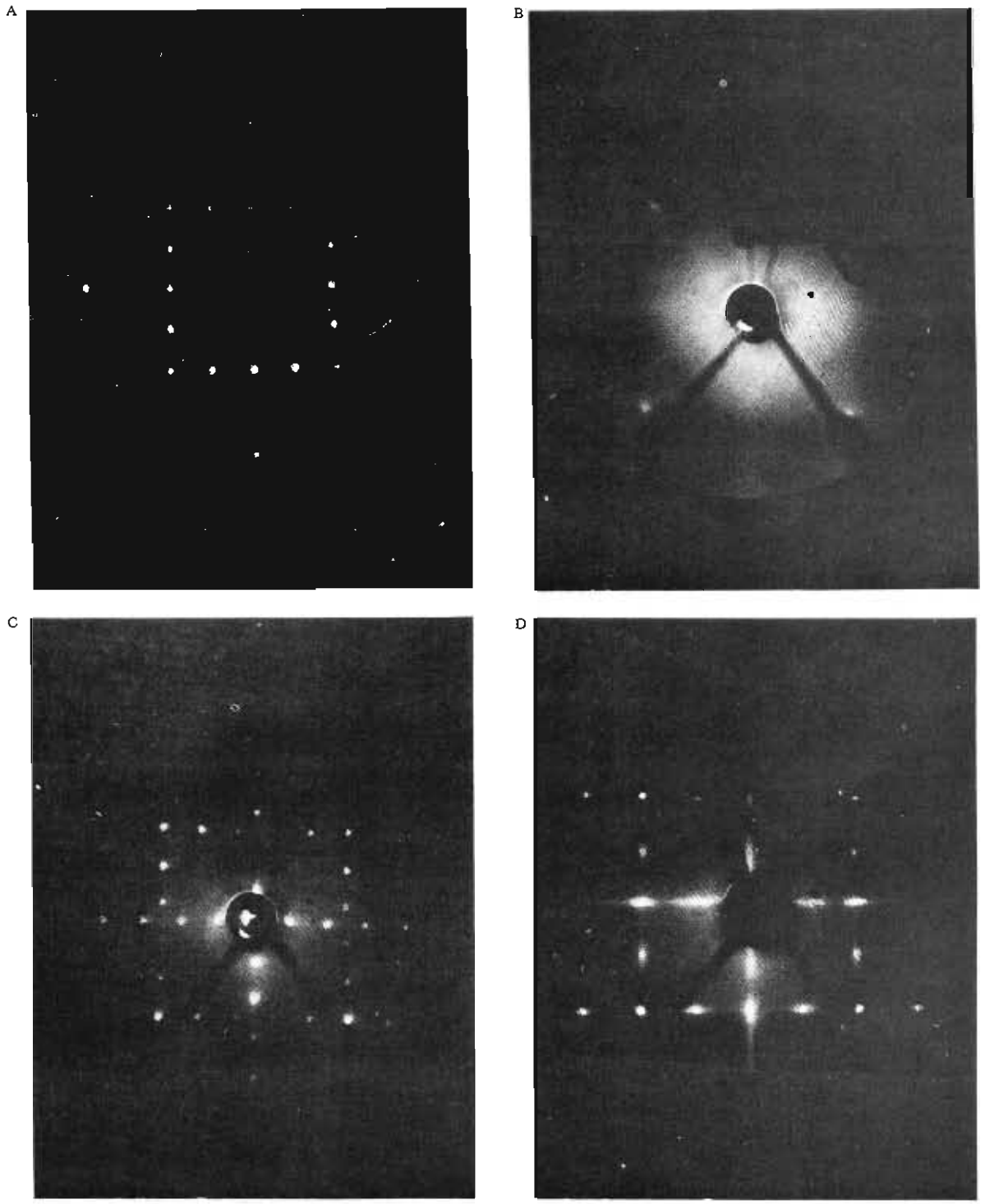

Figure 1. LEED patterns: (A) Pt(100)[$c(\sqrt{2}\times 2\sqrt{2})$]R45°–I, $\theta_I = 0.50$; (B) surface in part A after one cycle of electrochemical oxidation (1.2 V) and reduction (0 V) in 1 M perchloric acid saturated with iodine; (C) Pt(100)[$c(\sqrt{2}\times 5\sqrt{2})$]R45°–I, $\theta_I = 0.63$; (D) Pt(100)(incommensurate)R45°–I, $\theta_I = 0.52$.

For example, deposition of silver onto the Pt(100)[$c(\sqrt{2}\times 2\sqrt{2})$]R45°–I[5e] adsorbed lattice took place in two narrow voltammetric peaks to form two new superlattice structures.[4] In contrast, deposition of silver onto an incommensurate iodine layer (ordered without specific registry of the iodine layer to the platinum surface) produced broad voltammetric peaks and somewhat diffuse electrodeposited structures.[4] The nomenclature of surface crystallography has been discussed by Wood.[6]

In the present studies, the electrode surface was purposely disordered by electrochemical oxidation and reduction by using procedures such as those commonly employed to clean or "activate" platinum electrodes. A simple method for restoring the electrode surface to a well-defined state (without the necessity of ultrahigh-vacuum equipment) will be described. This method, which involves programmed heating of a Pt(100)

(5) (a) G. A. Garwood, Jr., and A. T. Hubbard, *Surf. Sci.*, **92**, 617 (1981); (b) J. A. Schoeffel and A. T. Hubbard, *Anal. Chem.* **49**, 2330 (1977); (c) R. M. Ishikawa and A. T. Hubbard, *J. Electroanal. Chem. Interfacial Electrochem.* **69**, 317 (1976); (d) R. M. Ishikawa, J. Y. Katekaru, and A. T. Hubbard, *ibid.*, **86**, 271 (1978); (e) T. E. Felter and A. T. Hubbard, *Surf. Sci.*, **112**, 281 (1981).

(6) E. A. Wood, *J. Appl. Phys.*, **35**, 1306 (1964).

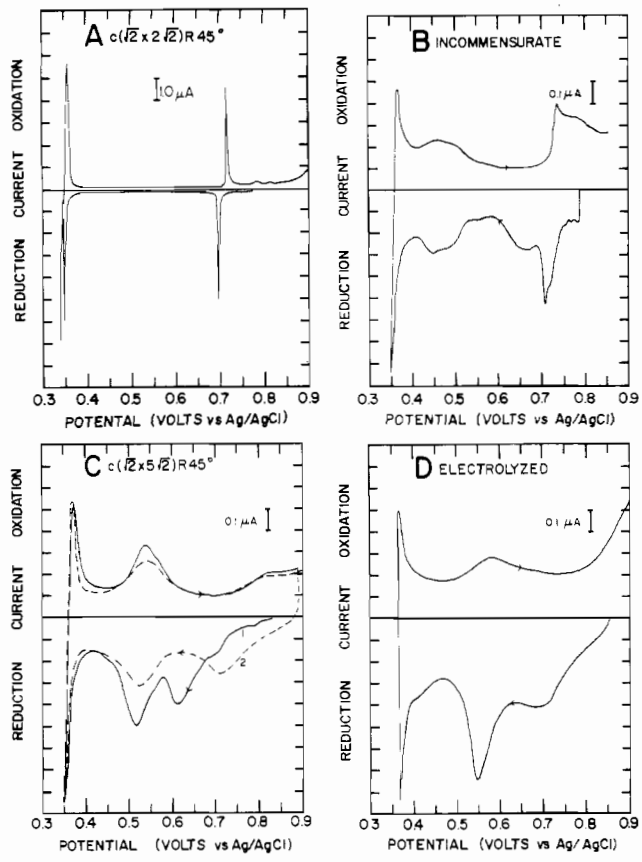

Figure 2. Cyclic current–potential curves for deposition of silver onto iodine adlattices: (A) Pt(100)[$c(\sqrt{2}\times2\sqrt{2})$]R45°–I, $\theta_I = 0.50$; (B) Pt(100)(incommensurate)R45°–I, $\theta_I = 0.52$; (C) Pt(100)[$c(\sqrt{2}\times5\sqrt{2})$]R45°–I, $\theta_I = 0.63$; (D) disordered surface as in Figure 1B.

monocrystal under an argon atmosphere containing iodine vapor, reproducibly produces a variety of iodine adlattices. This basic approach should be applicable to a wide range of metals and adsorbates. In the following we will compare the structure, composition, and electrochemical behavior of adsorbed and electrodeposited layers of iodine and silver on Pt(100) obtained by this simple method with those produced under ultrahigh vacuum.

Results and Discussion

In previous work it was found that the Pt(100)[$c(\sqrt{2}\times2\sqrt{2})$]R45°–I adlattice is stable in aqueous perchlorate electrolytes at open circuit but is removed by strong electrochemical oxidation, leaving a disordered oxygenous layer.[4,5e] The effect of electrochemical redox is illustrated by the LEED patterns shown in Figure 1A,B. Electrodeposition of silver onto the "$2\sqrt{2}$" iodine adlattice produced the sharply defined cyclic voltammogram shown in Figure 2A. Peaks 1 and 2 occurred at potentials (0.70 and 0.35 V) more positive than that for deposition of bulk silver (0.3 V); that is, "underpotential deposition" occurs. The heights and areas of peaks 1 and 2 are proportional to scan rate and electrode area; each corresponds to formation of specific AgI layer structures, as described in ref 4. In contrast, the voltammogram for deposition of silver onto the disordered surface is entirely different, a featureless trace giving no indication of the superlattice peaks observed with the "$2\sqrt{2}$" adlattice (Figure 2D).

After the disordered surface (Figure 1B) was heated with iodine as described in the Experimental Section, the $c(\sqrt{2}\times5\sqrt{2})$R45° LEED pattern shown in Figure 1C, reported here for the first time, was obtained. Accordingly, *the disordered surface has been converted to an ordered one by a simple treatment with iodine vapor under an atmosphere of argon.* The Auger spectrum obtained for this surface appears in

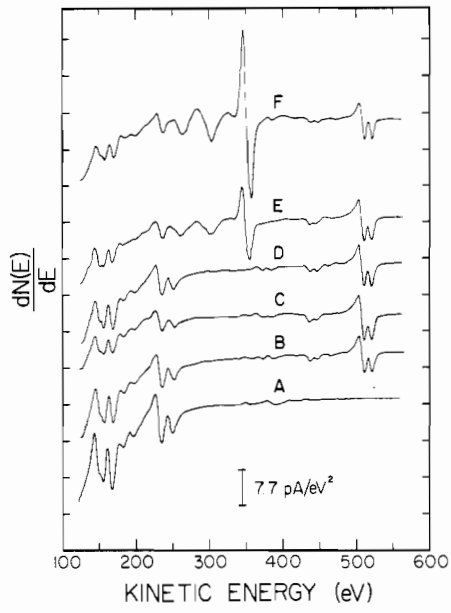

Figure 3. Auger spectra: (A) clean-surface Pt(100); (B) Pt(100)[$c(\sqrt{2}\times2\sqrt{2})$]R45°–I, $\theta_I = 0.50$; (C) disordered surface as in Figure 1B; (D) Pt(100)[$c(\sqrt{2}\times5\sqrt{2})$]R45°–I, $\theta_I = 0.63$; (E) silver electrodeposition on Pt(100)[$c(\sqrt{2}\times5\sqrt{2})$]R45°–I; (F) silver electrodeposition on Pt(100)[$c(\sqrt{2}\times2\sqrt{2})$]R45°–I.

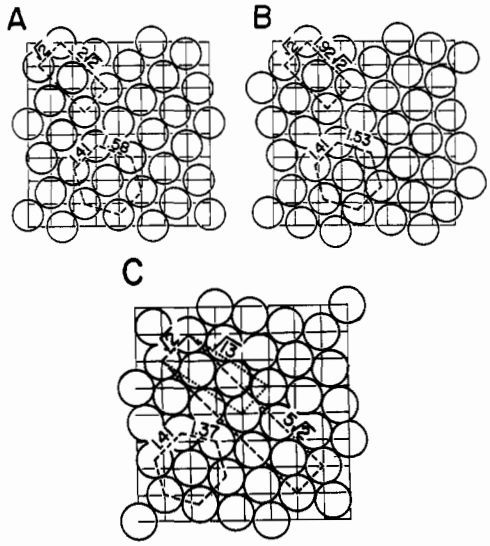

Figure 4. Surface structures: (A) Pt(100)[$c(\sqrt{2}\times2\sqrt{2})$]R45°–I, $\theta_I = 0.50$; (B) Pt(100)(incommensurate)R45°–I, $\theta_I = 0.52$; (C) Pt(100)[$c(\sqrt{2}\times5\sqrt{2})$]R45°–I, $\theta_I = 0.63$.

Figure 3. Integration of the spectrum[5b] indicates an iodine packing density, θ_I, of 0.63. A model structure having this centered rectangular ($\sqrt{2}\times5\sqrt{2}$) unit mesh rotated 45° from the Pt mesh and containing essentially the correct packing density of iodine atoms in the virtually hexagonal array expected[5a,c] for such a structure is shown in Figure 4C. The I–I interatomic distances in this structure, 3.81 and 3.93 Å, are noteworthy for being significantly less than the van der Waals distance, 4.3 Å. Such packing densities, greater than those predicted from van der Waals distances,[7] were not observed when adsorption was carried out under vacuum conditions.[4] The origins of this structure provided a helpful clue as to its nature: the LEED pattern of this structure (Figure 1C) is related to that (Figure 1D) of the preceding "incommensurate" structure (Figure 4B) by a mere coalescence

(7) L. C. Pauling, "Nature of the Chemical Bond", 3rd ed., Cornell University Press, Ithaca, NY, 1960.

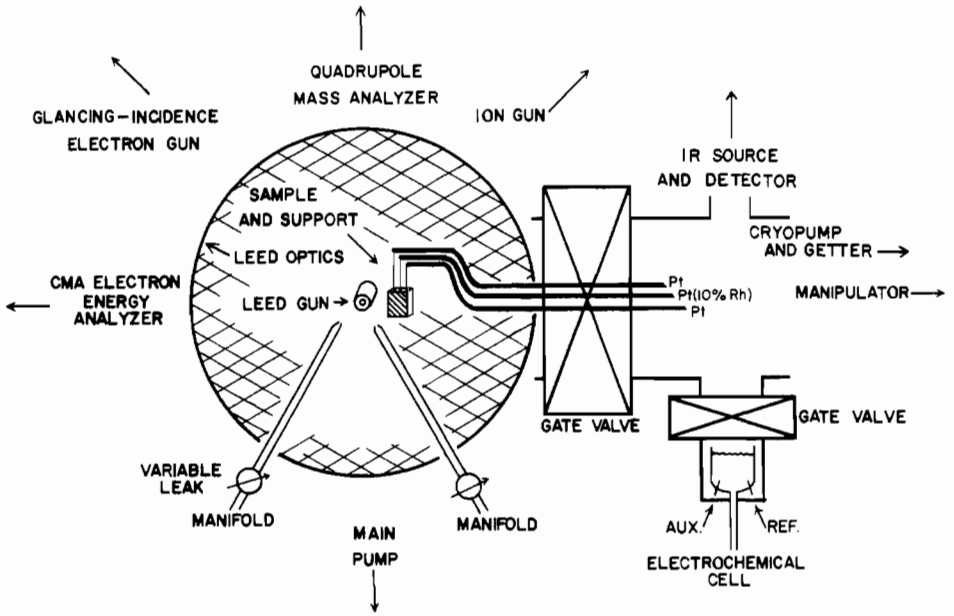

Figure 5. Schematic of LEED–electrochemistry instrument.

of the streaks located near half-index positions into sharp spots at the corresponding fifth-index positions. We also found that this Pt(100)[$c(\sqrt{2}\times5\sqrt{2})$]R45°–I adlattice occurs when the same procedure is applied to any of the iodine structures obtained under vacuum.

Thermal desorption from the "$2\sqrt{2}$" adlattice, monitored by mass spectroscopy and LEED, revealed that the desorption process encompasses a series of structural transitions at temperatures well above room temperature: $c(\sqrt{2}\times2\sqrt{2})$R45° → "hexagonal" → $c(2\times4)$ → disordered → Pt(100)-["complex"], as described in ref 5e. On the other hand, desorption from the "$5\sqrt{2}$" adlattice begins near room temperature: $c(\sqrt{2}\times5\sqrt{2})$R45° → (incommensurate)R45° → $c(\sqrt{2}\times2\sqrt{2})$R45°; from the "$2\sqrt{2}$" structure onwards, the series of structures was the same as before. Comparison of the I_2 (254 amu) and I (127 amu) signals during desorption with those for I_2 vapor ($I:I_2 = 5:1$) suggested that desorption from the "$5\sqrt{2}$" adlattice near room temperature yields primarily molecular I_2;[4] desorption from the "$2\sqrt{2}$" adlattice produced exclusively I atoms.[5e]

In the present work we have found that these *thermally induced structural transitions can also be made to occur at atmospheric pressure*. For instance, when the "$5\sqrt{2}$" surface was heated briefly to 365 °C under an iodine-free argon atmosphere, the Pt(100)[$c\sqrt{2}\times2\sqrt{2}$)]R45°–I structure was formed (Figure 4A). *The presence of this "$2\sqrt{2}$" structure is easily detectable voltammetrically (that is, without LEED equipment)* due to its distinctive silver deposition signature shown in Figure 2A. Silver deposition and dissolution at this surface are "structurally reversible". That is, structures present during dissolution were the same as those at comparable silver packing density during deposition. Multiple cycles gave identical voltammetric traces apart from a small decrease in peak height, provided that oxidative dissolution of adsorbed iodine was not made to occur.

Extreme sensitivity of silver electrodeposition to the structure of the iodine adlattice (and therefore the uniqueness of the voltammetric signature described above) is indicated by the voltammetric trace for deposition onto the Pt(100)(incommensurate)R45°–I surface (Figure 2B). The "incommensurate" layer differs from the preceding "$2\sqrt{2}$" adlattice only by a slight compression of the iodine unit mesh (about 0.2 Å) along the "$2\sqrt{2}$" edge; the platinum substrate has the ideal Pt(100)(1×1) structure in both cases. Voltammetric peaks for silver deposition onto this surface were more numerous, occurred at different potentials, and were broader by a factor of 10 than those obtained with the "$2\sqrt{2}$" adlattice. Evidently, most of the adsorbed I atoms were unable to participate in the formation of a AgI(100) monolayer and instead reacted with the deposited silver to form polycrystalline AgI. Silver deposited subsequently forms a disordered layer of Ag atoms beneath the AgI layer, based upon Auger intensity decreases for Pt, increases for Ag, and constancy for iodine, as well as increasing diffuse LEED intensity and fading integral-index LEED beams.

The second voltammetric cycle for deposition of silver onto the densely packed "$5\sqrt{2}$" iodine adlattice was noticeably different from the first (Figure 2C) while subsequent cycles were similar to the second, indicating that material deposited during the first negative scan was unstable in some way. The Auger signal for silver deposited during the first negative scan was unexpectedly small (Figure 3E) while those for subsequent cycles resembled that for the "$2\sqrt{2}$" surface (Figure 3F). The Auger signal for iodine decreased sharply during the first deposition scan, approaching that for the "$2\sqrt{2}$" surface. Integral-index LEED beams (those due to the Pt(100) substrat) remained sharp after silver deposition. All LEED intensity attributable to Ag and I was diffuse during the first deposition scan but began to display the $(\sqrt{2}\times\sqrt{2})$R45° beams obtained for the "$2\sqrt{2}$" adlattice after subsequent scans. Evidently, silver electrodeposited onto the "$5\sqrt{2}$" adlattice reacted to form polycrystalline AgI, which gradually desorbed into the electrolyte, causing the progressive changes described. It is noteworthy that removal of part of the adsorbed iodine restored the ability of the surface to form a stable silver layer.

Experimental Section

The electrode was prepared from a platinum single crystal, cut and polished[8] in such a way that all six faces were crystallographically equivalent to Pt(100). Polishing was done with successively finer emery paper disks (18, 240, 320, 400, and 600 grit), lubricated with water, and diamond paste (6 and 0.25 μm), lubricated with kerosene. X-ray reflection photographs[9] were taken at each abrasive stage until removal of surface damage left by the previous stage was complete. On the basis of the appearance of the X-ray photographs[9] and the known characteristics of diamond lapping,[8] we estimate the depth of surface damage following polishing to be about 1000 Å. An electrochemical

(8) L. E. Samuels, "Metallographic Polishing by Mechanical Methods", Pitman, London, 1967.
(9) E. A. Wood, "Crystal Orientation Manual", Columbia University Press, New York, 1963.

etching procedure was found that largely removes this remaining damaged layer: Grube and Reindardt[10] reported that dissolution of platinum into hot hydrochloric acid was very efficient when the temperature was kept above 80 °C, the HCl concentration exceeded 7 M, and the current density was less than about 10^{-3} A/cm^2. When we repeated their experiment using lower current density (10^{-5} A/cm^2), we found that removal of platinum occurred quantitatively as they reported and produced far fewer etch pits than were observed at higher current densities, judging from optical and scanning electron microscopic examination of the surface. In our experiments, etching was employed to remove about 1000 Å of platinum, based upon four-electron oxidation of the metal to $PtCl_6^{2-}$. Removal of a similar amount of platinum by the conventional procedure involving the use of aqua regia resulted in greater pitting of the surface. The effect of lengthy ion bombardment and annealing after etching was to decrease the size of the LEED spots and the proportion of diffuse intensity somewhat, indicating an increase in the sizes of the ordered domains (for references to revies of LEED, see ref 1).

Instrumentation and procedures for combined LEED and electrochemistry have been described[1-5] and reviewed,[11] although slight modifications were made for the present work. A diagram of the apparatus appears in Figure 5. The Pt crystal was supported by a pair of fine Pt wires (0.40-mm diameter) spot-welded to one edge. Crystal temperature was measured by means of the thermoelectric voltage generated between a fine (0.25-mm diameter) 90% Pt-10% Rh wire (spot-welded to the crystal) and one of the support wires; this thermocouple voltage was distinguished from the (ac) heating voltage by use of an RC filter.

Electrolytic solutions were prepared from pyrolytically distilled water[12] and reagent grade chemicals. Compressed argon was obtained from Union Carbide Corp. Electrode potentials were measured with respect to a Ag/Ag$^+$ half-cell (10^{-3} M $AgClO_4$ in aqueous 1 M $HClO_4$) and reported relative to the Ag/AgCl half-cell (1 M NaCl), based upon direct measurements between the two reference half-cells. Conventional three-electrode potentiostatic circuitry based upon operational amplifiers was employed.

Pt(100)[$c(\sqrt{2}\times 2\sqrt{2})$]R45°-I. Preparation under Vacuum. A clean Pt(100) surface was treated for several minutes at 200 °C with an iodine-vapor beam (Figure 5) equivalent to 3×10^{-4} torr; the resulting incommensurate structure (Figure 4B) was removed from the iodine beam and heated to 350 °C. After it was allowed to cool to ambient temperature, the crystal was exposed to the iodine-vapor beam until the LEED pattern indicated that the $c(\sqrt{2}\times 2\sqrt{2})$R45°-I structure was present. The LEED pattern and structure are shown in Figures 1A and 4A. Auger spectral intensity for iodine was normalized to this structure, previously shown to contain one I atom per two surface Pt atoms, $\theta_I = 0.50$.[5e]

Pt(100)[$c(\sqrt{2}\times 5\sqrt{2})$]R45°-I. Preparation at Atmospheric Pressure. The platinum surface (either clean or iodine coated) was blanketed with a flowing argon atmosphere and placed at a distance of about 10 mm from crystals of iodine in a Pyrex glass container (substituted momentarily for the "electrochemical cell" in Figure 5); the distance was adjusted such that the Pt electrode was surrounded by visible I_2 vapor during heating. The electrode was heated electrically to 900 °C for 30 s and 400 °C for 3 min and allowed to cool to ambient temperature. The resulting structure (Figure 4C) contains $\theta_I = 0.63$ (calculated for Pt(100)[$c(\sqrt{2}\times 5\sqrt{2})$]R45°-I: $\theta_I = 0.60$). Programmed heating of this Pt(100)[$c(\sqrt{2}\times 5\sqrt{2})$]R45°-I adlattice under vacuum or iodine-free argon produced the Pt(100)(incommensurate)R45°-I structure (300 °C) and the Pt(100)[$c(\sqrt{2}\times 2\sqrt{2})$]R45°-I structure (365 °C). Both of these iodine adlattices are easily recognized by their distinctive current-potential curves. The other adlattice structures, derived from this "$2\sqrt{2}$" adlattice by partial desorption of iodine as described in ref 5e, were also obtained.

Acknowledgment. Acknowledgment is made to the National Science Foundation, the Air Force Office of Scientific Research, and the donors of the Petroleum Research Fund, administered by the American Chemical Society, for support of this research.

Registry No. Pt, 7440-06-4; Ag, 7440-22-4; AgI, 7783-96-2; I_2, 7553-56-2.

(10) G. Grube and H. Reinhardt, *z. Elektrochem.*, **37**, 307 (1931).
(11) (a) A. T. Hubbard, *Acc. Chem. Res.*, **13**, 1977 (1980); (b) A. T. Hubbard, *J. Vac. Sci. Technol.*, **17**, 49 (1980).
(12) B. E. Conway, H. Angerstein-Kozlowska, W. B. Sharp, and E. E. Criddle, *Anal. Chem.*, **45**, 1331 (1973).

Contribution from the Department of Chemistry, Purdue University, West Lafayette, Indiana 47907

A Two-Level Approach to Deconvoluting Absorbance Data Involving Multiple Species. Applications to Copper Systems

CYNTHIA E. ATKINS, STEVEN E. PARK, JUDITH A. BLASZAK, and DAVID R. McMILLIN*

Received June 1, 1983

A least-squares algorithm for obtaining stability constants and molar absorptivities from absorbance data is described. The stability constants are refined by a numerical search method. At each stage in the refinement of the stability constants, conditionally optimum values of the molar absorptivities are estimated by a standard linear least-squares procedure. Treating the parameters on two different levels in this way reduces the guesswork involved and increases the likelihood of converging upon the minimum in the error surface. The method is used to characterize a pentakis complex of imidazole with copper(II) in aqueous solution that exhibits $\lambda_{max} = 650$ nm where $\epsilon = 118$ M^{-1} m^{-1}. In a second study the mono- and bis-ligand complexes of 2,9-dimethyl-1,10-phenanthroline with copper(I) are characterized in acetonitrile. Here, the most interesting findings are that the mono and bis complexes exhibit charge-transfer absorption maxima at very different wavelengths and that the intensities are not simply related one to the other.

Introduction

In the course of our work on copper complexes in solution we have often been concerned with speciation and spectral properties.[1,2] Consequently we have developed a method for deconvoluting stability constants and absorption spectra using absorbance data from solutions containing multiple species. Here, we describe the program and analyze two systems; in each case it is necessary to qualify previous conclusions drawn in the literature. Whereas previous polarographic studies have suggested that a maximum of four imidazole ligands coordinate to Cu(II),[3] we observe a red shift in the visible spectrum at high imidazole/Cu(II) ratios. This result is reminiscent of the well-known pentaamine effect[4] and shows that at least five imidazole ligands can bind to Cu(II). In studies of com-

(1) Blaszak, J. A.; McMillin, D. R.; Thornton, A. T.; Tennent, D. L. *J. Biol. Chem.* **1983**, *258*, 9886-9892.
(2) Rader, R. A.; McMillin, D. R.; Buckner, M. T.; Matthews, T. G.; Casadonte, D. J.; Lengel, R. K.; Whittaker, S. B.; Darmon, L. M.; Lytle, F. E. *J. Am. Chem. Soc.* **1981**, *103*, 5906-5912.
(3) Li, N. C.; White, J. M.; Doody, E. *J. Am. Chem. Soc.* **1954**, *76*, 6219-6223.
(4) Hathaway, B. J.; Tomlinson, A. A. G. *Coord. Chem. Rev.* **1970**, *5*, 1-43.

0020-1669/84/1323-0569$01.50/0